01

Brillouin-Mandelstam scattering in weakly disordered nanoparticles

© A.G. Yashenkin,[1,2] O.I. Utesov,[3] S.V. Koniakhin[3,4]

[1]St. Petersburg State University, Faculty of Physics,
198504 Old Peterhof, Saint Petersburg, Russia
[2]St. Petersburg Nuclear Physics Institute, National Research Center „Kurchatov Institute,“
188300 Gatchina, Russia
[3]Institute for Basic Science,
34126 Daejeon, South Korea
[4]Basic Science Program, University of Science and Technology,
34113 Daejeon, South Korea
e-mail: ayash@mail.ru

Received November 24, 2024
Revised November 24, 2024
Accepted November 24, 2024

Utilizing the earlier elaborated general approach we undertook the comprehensive analisys of model light scattering spectra in arrays of nanoparticles on nonpolar crystals within Brillouin-Mandelstam and Raman channels. It is shown that the light scattering by acoustic phonons could serve as an independent tool with respect to the main Raman one providing us with additional experimental information – particularly, about the properties of nanoparticles sufaces.

Keywords: Raman and Brillouin-Mandelstam light scattering, acoustic phonons, nanoparticles, nonpolar crystals.

DOI: 10.61011/TP.2025.03.60848.351-24

Introduction

The significant progress achieved over the last two decades in physicochemical studies of nanosystems and, especially, in their numerous and diverse high-tech applications has drawn close attention to the development of reliable methods for monitoring the properties, standardization, and certification potential of these systems. For all the richness and diversity of such systems, of particular interest are zero-dimensional objects — nanoparticles (see, e.g., review [1] and references therein). This is attributable both to the relative simplicity of their production (e.g., in the form of quantum dots, including semiconductor ones; crystalline nanopowders, such as much-studied nanodiamonds, including detonation ones; suspensions; etc.) and to a variety of potentially applicable exotic properties of nanoparticles distinguishing them from a macroscopic solid, which stem primarily from their high surface/volume ratios and the dimensional quantization of certain physical quantities (e.g., momentum) in these systems.

Various methods are used at present to examine the properties of nanoparticles and their arrays; in this context, optical methods, being non-destructive, accurate, and relatively inexpensive, appear to be particularly promising. Owing to the extreme smallness of the objects being studied, the optical effect best suited for such research is Raman scattering. Specifically, the approach to processing of Raman spectra of weakly disordered nonpolar nanocrystals (primarily nanodiamonds) developed in our recent studies [2,3] provided an opportunity to extract such parameters as the size of particles in a nanopowder, their dispersion and shape, and the degree of their contamination from experimental data with high accuracy. In addition, this approach provided an opportunity to explain theoretically the known experimental 1/L dependence of the Raman peak width on the particle size, which was observed by Yoshikawa [4]. In this case, the magnitude of broadenings matching those observed experimentally for relatively pure diamonds was provided by the mere inclusion of disorder in the form of a small concentration of point defects (see below) that corresponds, in particular, to the experimentally measured concentrations of nitrogen and NV- defects in diamond nanoparticles. A very close fit to the experimental data for particles in the nanometer range was obtained within this approach (see the references in [5]); in fact, it is much better than the one provided by the widely used empirical method of phonon confinement [6,7].

As for Brillouin-Mandelstam (BM) scattering in nanoparticles, it cannot be said that the corresponding experiments have not been performed at all (see, e.g., [8,9]), but they are much less numerous than Raman ones. BM scattering is traditionally used to study the physicochemical structure of matter, while the Raman effect is used primarily to examine collective excitations of solids.

The present study was motivated by the publishing of report [9] containing detailed data on BM scattering in nanoparticles and by the opinion expressed in [8,9] that Raman scattering of acoustic phonons in nanoparticles may be used to study them and is potentially even better suited for this than the common Raman effect. We thought it appropriate to carry out an in-depth analysis of BM spectra similar to the one performed for the Raman effect [2,3]

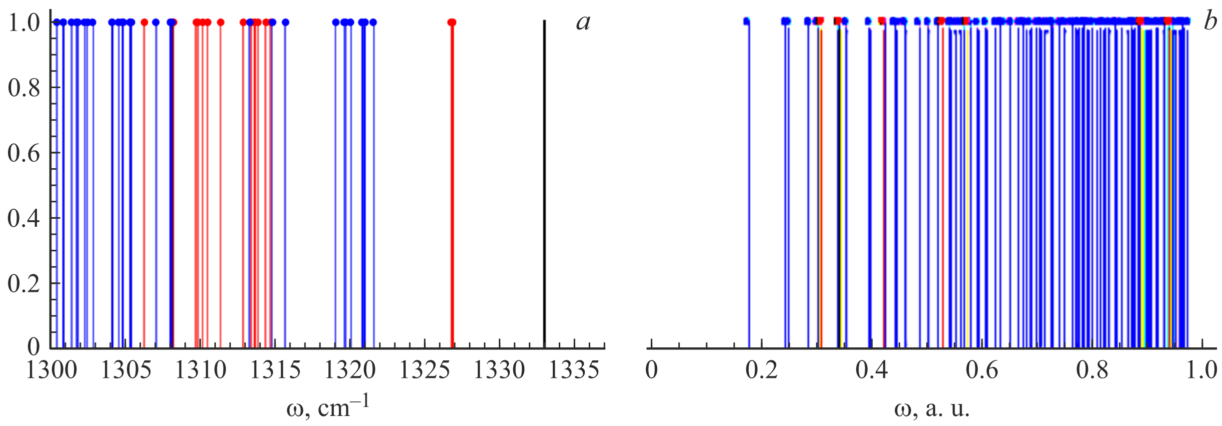

Figure 1. Raman (*a*) (taken from [13]) and BM (*b*) phonon spectra of a cubic particle. Active modes contributing to the corresponding experimental peaks are shown in red. In the Raman case, the structure of active modes is richer; a separate high-lying mode, which provides 2/3 of the total intensity, and a quasi-band separated from it, which is responsible for the asymmetry of the Raman peak, are seen. The BM spectrum has several active modes, and their properties are discussed in the text.

and compare the capabilities of both approaches. The verdict of our analysis is as follows: the specifics of BM scattering make it useful in certain aspects where Raman scattering provides a rather rough description of the dynamics of vibrational modes and, consequently, the structure of nanoparticles. Therefore, a BM experiment may serve as an informative complementary method and, combined with Raman spectroscopy, provide more complete and detailed data on nanoparticles and their arrays.

1. Phonon spectra. „Active“ and „silent“ modes

Let us start our comparative analysis by calculating the vibrational eigenmodes in the optical (Raman) and acoustic (BM) cases. A significant difference becomes evident right from the onset. In the Raman case, eigenmodes are found both within the atomistic (discrete) theory via the dynamic matrix diagonalization method (DMM) [2] and within the continuum approach by solving the Dirichlet problem for the Klein–Fock–Gordon equation in Euclidean space (EKFG) [3] for a particle. As for the acoustic mode, only the first option remains well-defined at an arbitrary particle shape. The continuum theory needs to be supplemented by Neumann-type conditions for the radial part of derivative of the eigenfunction at the boundary of the region where, in the general case, modes (and polarizations) become entangled and, consequently, the boundary conditions are ambiguous for all particle shapes except the spherical one. Therefore, we rely mostly on DMM in subsequent calculations, but borrow the notation from the spherical continuum problem. Details of the solution of the mathematical problem of vibrational modes of a spherical particle in the elastic continuum model, the notation of these modes stipulated by symmetry arguments, and an account of the application of this model to the problem of BM scattering were provided in [10–12].

We investigated numerically a simple cubic lattice with nearest and next-nearest neighbor interactions within the „mass on springs“ model. Figure 1 shows the phonon spectra for the Raman and BM problems. It is clear that the spectrum is quite rich in both cases. At the same time, most eigenfrequencies do not contribute to the optical response, since their matrix elements of interaction with a photon, which are specified by the squared modulus of the eigenfunction (or its derivative) integrated over the volume of a nanoparticle, are close to zero for symmetry reasons. Let us consider, for example, the spectra of active modes of cubic and spherical particles in Fig. 2. Only two modes, which are identified as the first breathing (B-mode with azimuthal quantum number $l = 0$) and the first quadrupole (Q-mode with $l = 2$) vibrational modes of a spherical particle, make a significant contribution to the intensity; therefore, the other three lines in the figure (these are satellites of the first breathing and quadrupole modes) may be neglected at the start. It is proven below that the notation of eigenmodes of a sphere may be transferred with little to no changes to particles with a small number of faces (at least for Platonic and Archimedean solids).

2. Dependence of frequencies on the shape and size of particles

It is easy to plot similar graphs for particles with a number of faces falling within the range between a cube and a sphere. We did this for particles in the form of an octahedron with $p = 8$ faces and a truncated octahedron with $p = 14$. The phenomena we observed in the process of examination of a cube and a sphere (as p decreases, the frequencies of Q- and B-modes converge, the intensity is transferred from the breathing mode to the quadrupole one,

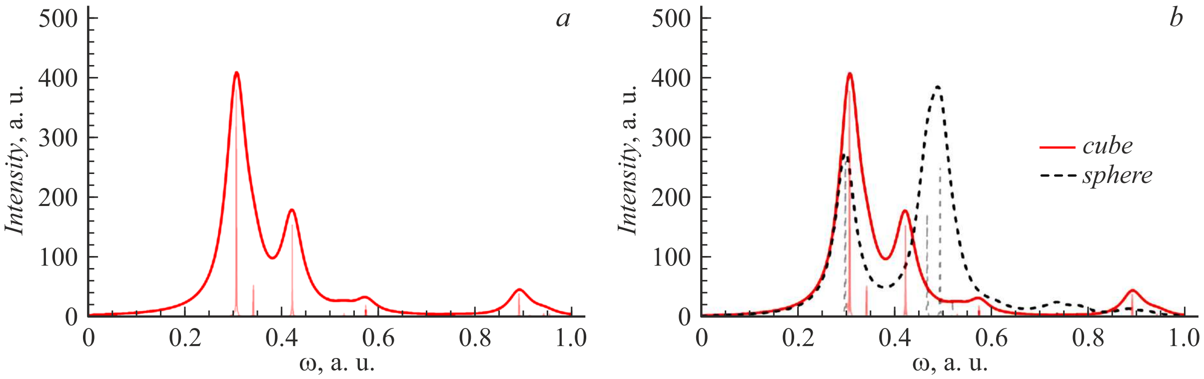

Figure 2. Active BM modes of the spectrum of a cubic particle (red solid curve) (*a*) and comparison of active modes of a cubic (red solid curve) and spherical (black dotted curve) particles (*b*); the curves are broadened artificially for clarity. In both cases, the breathing mode is located to the right of the quadrupole one. It is evident that the position of the quadrupole mode is almost independent of the particle shape, although its intensity decreases slightly with an increase in the number of faces. At the same time, breathing mode shifts to the right, and its intensity increases. The total intensity of peaks is determined primarily by the Q-mode for both the cube and the sphere; in the latter case, a second quadrupole doublet is added to the first one.

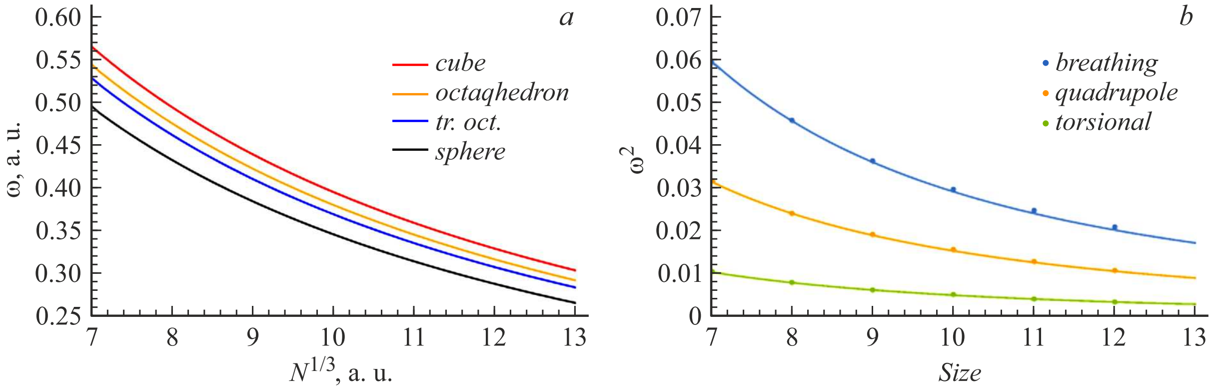

Figure 3. Dependence of frequencies of active Q-modes of nanoparticles on the shape (*a*) and size of a (cubic) particle (*b*). Here, N is the particle volume. To demonstrate the scale of the dimensional quantization effect and for comparison with the Raman case, the silent torsional mode (as the lowest-energy mode of the acoustic spectrum) is also shown in panel *b*.

and the second quadrupole doublet is amplified) were found to persist at intermediate values of p and are characterized by a certain function that changes approximately by 12% with a variation in shape (see Fig. 3, *a*; for comparison, the frequencies of Raman lines vary with shape by 20%). In other words, a description of non-spherical particles in terms of modes inherent, strictly speaking, to a sphere only is also meaningful, since these modes have a common symmetric origin. The trend toward an increase in significance of the contribution from higher quadrupole harmonics with an increase in the number of nanoparticle faces is preserved in this case.

Another important dependence, which was confirmed numerically, is the inverse dependence of frequencies of active modes on particle size L that follows from the acoustic nature of these excitations (see Fig. 3, *b*):

$$\omega_{n,l}(L, p) \approx u(p, n, l)a^{-1}(a/L), \tag{1}$$

where n is the principal quantum number of the mode, u is its velocity, a is the lattice constant, and L is the nanoparticle size (in the case of a cubic particle, the cube edge length). Note that formula (1) provides an opportunity to determine experimentally the size of nanoparticles based on the BM peak position.

3. Broadening of phonon lines due to disorder

The processes of scattering of optical phonons by spatial inhomogeneities of a crystal played a significant role in the formation of the Raman peak. „Disorder“ was (and is) understood as the following model scenarios: (a) rare point mass defects at sites, both strong (the mass of a defect atom differs greatly from the mass of carbon) and weak, where the rarity of defects (lack of interference between the events of scattering by individual defects) is ensured by the smallness of dimensionless disorder strength

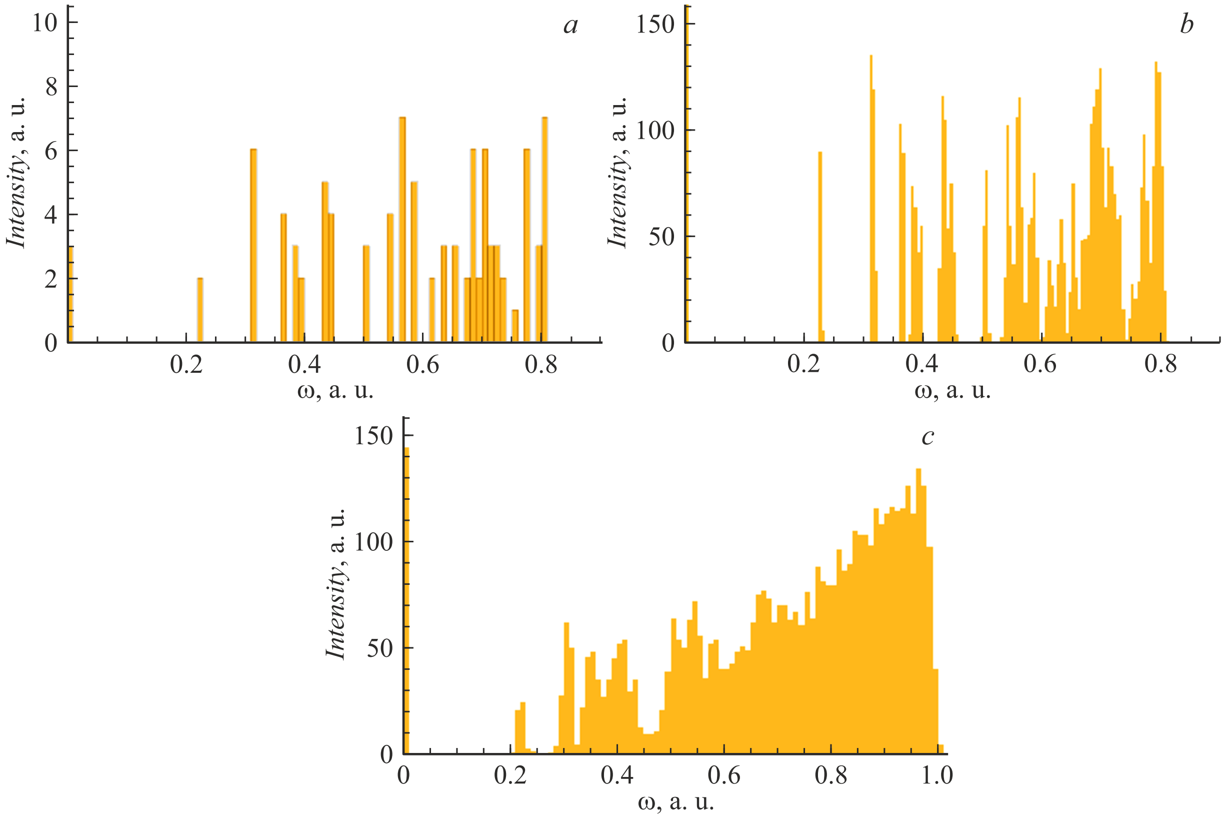

Figure 4. Density of states of weakly disordered acoustic modes in a nanoparticle with bulk weak (*a*), fairly strong ($S = 0.04$) (*b*), and surface (10 % of surface vacancies) (*c*) disorder.

parameter $S \ll 1$ (note that a value of $S \sim 0.003$ already provides fairly large Raman peak widths compatible with the experimental ones); (b) the same scenario with a point interatomic bond defect („spring“) K_{ij}; (c) extended and resonance defects, still with a small value of $S \ll 1$ due to the smallness of concentration. Such media are referred to as „weakly disordered“ ones. It is evident that the effects of diamond amorphization are beyond the scope of analysis, since the concentration of inhomogeneities in this case is on the order of unity, although the amplitude of scattering by a single defect may be small.

A fairly strong attenuation of phonons in a weakly inhomogeneous medium ensured a finite peak width that is comparable to the experimental one [4,13,14]. The primary contribution was provided by bulk disorder, while the surface of nanoparticles produced only a small subleading contribution [13,14]. Scattering by disorder has been examined in [13,14] both analytically and numerically, and an impressively accurate agreement between these two approaches was achieved.

And what of the broadening of acoustic phonon lines in the case of BM scattering? Let us first consider analytically the scattering of acoustic phonons by point mass defects distributed in the bulk of a nanoparticle. As in Raman scattering, two scenarios, which differ somewhat in the computational approach, should be distinguished: the case of non-overlapping phonon lines and the case of a continuous spectrum (where overlapping is provided by disorder). With separated lines, attenuation Γ is given by

$$\Gamma_{nl} \simeq S^{1/2}\,(a/L)^{5/2}\,f(n,l,p),$$

where parameter $S = n_{imp}(\delta m/m)^2$ is a measure of the disorder strength and f is a certain function that depends on the shape of nanoparticles and quantum numbers of the mode and increases rapidly with these numbers (from values on the order of unity for the first quantum numbers). Here, n_{imp} is the concentration of point impurities exemplified by substitutional impurities with mass defect δm relative to mass m of atoms of a regular lattice.

In the contrary case of overlapping levels, we find

$$\Gamma_{nl} \simeq S\,(a/L)^4\,g(n,l,p),$$

where g is another function from the same class as f.

It is evident that, in contrast to optical phonons (which, to remind [13,14], had $\Gamma \propto S^{1/2}(a/L)^{3/2}$ for separated levels and $\Gamma \propto S(a/L)$ for overlapping ones), acoustic phonons feature a weak attenuation due to scattering by bulk disorder, since it is proportional to higher powers of small parameter a/L. The results of the numerical experiment illustrated in Figs. 4, *a, b* suggest the same conclusion. These figures present the density of states of disordered acoustic

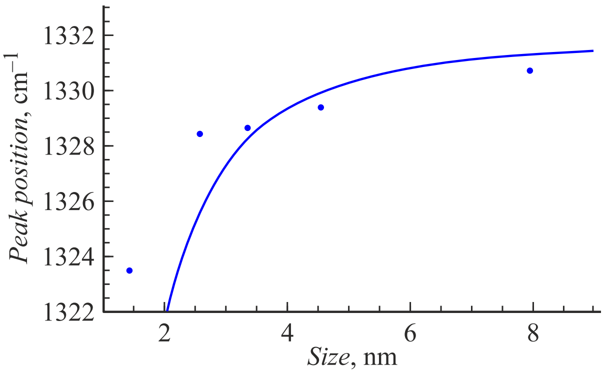

Figure 5. Fit to the Raman experiment performed in [9] with corrected values of fitting parameters.

phonons at two different values of disorder strength S; the first is extremely small, while the second is so large that the levels of optical phonons should overlap to the utmost extent. In the present case, weaker disorder takes the form of completely separated levels, while the spectrum at the second (larger) value is just barely starting to overlap at high quantum numbers. Therefore, bulk disorder has little effect on the BM spectrum.

The pattern changes significantly if we introduce surface defects into analysis. This case is presented in Fig. 4, *c*. It can be seen that even at a relatively low concentration of surface vacancies, the density of states of acoustic phonons is a continuous function (levels overlap). Thus, BM spectra are extremely sensitive to surface disorder, but have a relatively weak sensitivity to bulk disorder; i.e., the pattern is the exact opposite of the Raman one. This is why, in our view, it is beneficial to use these two methods together: they naturally complement each other.

4. Discussion

Another important aspect of our research should be mentioned in conclusion. In the already mentioned study [9], Stehlik et al. have attempted to fit their experimental data (the data on Raman scattering in nanoparticles included) using various theoretical constructs, including our theory presented in [2,3]. By an unfortunate coincidence, the parameter values for fitting were taken from an earlier work [15], where (just once!) an incorrect numerical multiplier was specified. A fit with corrected parameter values, which characterizes the experimental data from [9] much better, is presented in Fig. 5.

The theory presented here will be discussed in detail in a separate in-depth paper.

Thus, the process of Raman scattering of light by acoustic phonons (BM effect) in weakly disordered crystalline nanoparticles (i.e., at low defect concentrations) was analyzed and modeled thoroughly. Optically active phonon modes (breathing and quadrupole ones) were identified, and the dependences of frequencies and intensities of their lines on the size and shape of nanoparticles were analyzed. It was demonstrated that the broadening of phonon lines of these modes is largely insensitive to bulk disorder in a particle, but depends strongly on surface defects. Thus, BM scattering may serve as an experimental nanoparticle examination technique complementary to the Raman effect.

Conflict of interest

The authors declare that they have no conflict of interest.

References

[1] V.N. Mochalin, O. Shenderova, D. Ho, Y. Gogotsi. Nature Nanotechnol., **7**, 11 (2012). DOI: 10.1038/NNANO.2011.209

[2] S.V. Koniakhin, O.I. Utesov, I.N. Terterov, A.V. Siklitskaya, D. Solnyshkov, A.G. Yashenkin. J. Phys. Chem. C, **122**, 19219 (2018). DOI: 10.1021/acs.jpcc.8b05415

[3] O.I. Utesov, A.G. Yashenkin, S.V. Koniakhin. J. Phys. Chem. C, **122**, 22738 (2018). DOI: 10.1021/acs.jpcc.8b07061

[4] M. Yoshikawa, Y. Mori, H. Obata, M. Maegawa, G. Katagiri, H. Ishida, A. Ishitani. Appl. Phys. Lett., **67**, 694 (1995). DOI: 10.1063/1.11.115206

[5] S.V. Koniakhin, O.I. Utesov, A.G. Yashenkin. Diamond and Related Materials, **146**, 111182 (2024), DOI: 10.1016/j.diamond.2024.111182

[6] H. Richter, Z. Wang, L. Ley. Solid State Commun., **39**, 625 (1981). DOI: 10.1016/0038-1098(81)90337-9

[7] I. Campbell, P.M. Fauchet. Solid State Commun., **58**, 739 (1986), DOI: 10.1016/0038-1098(86)90513-2

[8] F. Kargar, A.A. Balandin. Nature Photonics, **15**, 720 (2021). DOI: 10.1038/s41566-021-00836-5

[9] A. Vlk, M. Ledinsky, A. Shiryaev, E. Ekimov, S. Stehlik. J. Phys. Chem. C, **126**, 6318 (2022). DOI: 10.1021/acs.jpcc.2c00446

[10] N. Nishiguchi, T. Sakuma. Solid State Commun., **38**, 1073 (1981). DOI: 10.1016/0038-1098(81)90020-x

[11] M. Fujii, T. Nagareda, S. Hayashi, K. Yamamoto. Phys. Rev. B, **44**, 6243 (1991). DOI: 10.1103/PhysRevB.44.6243

[12] E. Duval. Phys. Rev. B, **46**, 5795 (1992). DOI: 10.1103/PhysRevB.46.5795

[13] S.V. Koniakhin, O.I. Utesov, A.G. Yashenkin. Phys. Rev. B, **102**, 205422 (2020). DOI: 10.1103/PhysRevB.102.205422

[14] O.I. Utesov, A.G. Yashenkin, S.V. Koniakhin. Phys. Rev. B, **102**, 205421 (2020). DOI: 10.1103/PhysRevB.102.205421

[15] A.P. Meilakhs, S.V. Koniakhin. Superlattices Microstruct., **110**, 319 (2017).

Translated by D.Safin